

# Patterning of Multi-slits on Pipes for Developing Fine Diameter Stents

Toshiyuki Horiuchi, Hiroshi Sakabe and Hiroshi Kobayashi

Graduate School of Engineering, Tokyo Denki University, 5 Senju-Asahi-cho, Adachi-ku, Tokyo, Japan

**Keywords:** Stent, Laser Scan Lithography, Slit Pattern, Etching, Stainless Steel Pipe.

**Abstract:** Precise slit patterns were delineated on fine stainless steel pipes with an outer diameter of 100  $\mu\text{m}$ . The aim of the research is to clarify the feasibility of fabricating stents with diameters of less than 1 mm by delineating precise multi-slit patterns on fine pipes. Using a laser scan exposure system, slit patterns with widths of 11-29  $\mu\text{m}$  were successfully delineated as fundamental stent patterns. At first, the exposure shutter was opened just before the specimen was scanned. However, swells appeared at the pattern ends. For this reason, exposure program was changed to open the shutter after starting the specimen scan. As a result, swells were completely diminished. In addition to simple parallel slit patterns, alternatively positioned parallel slit patterns were homogeneously delineated. Because the delineation speed of the investigated method is not fast, an idea of scan projection lithography was also proposed. It is feasible to fabricate stents if the pipes are etched using the resist patterns as etching masks continuing to the lithography.

## 1 INTRODUCTION

Catheters and stents have become very important operation tools and medical components for low invasive cures of diseased circular organs, blood vessels, ureters, and others. Speaking on the stents, net like structures with very complicated patterns have been proposed and used. (Baichoo and Wong Kee Song, 2014; Chandrasekhar et al., 2014; Consentino et al., 2014; Hanada et al., 2013; Kumar et al., 2013; Wang et al., 2014; Zhu et al., 2013) Such structures were conventionally fabricated by weaving fine wires or precisely cutting pipes by a focused laser beam, and typical outer diameter were 2-3 mm.

It is considered that stents with finer diameters for example 0.5-1 mm are also necessary in some cases. However, it will be difficult to fabricate stents with such fine diameters using the conventional methods. For this reason, a new fabrication method of fine-diameter stents is proposed here, and the feasibility of the method is investigated.

In the new method, it is supposed that net-like patterns of stents are delineated by laser scan lithography onto fine stainless-steel pipes, and the pipes are etched to stents. It has already been demonstrated in past researches that various helical patterns are surely delineated onto fine pipes or

wires with diameters down to several tens microns. (Horiuchi and Sasaki, 2012)

However, it is necessary to delineate more complicated patterns for fabricating net-like stents. The stents need to have net-like features that can be extended in the radial direction by a balloon inserted in the stents. On the other hand, they need to have appropriate rigidity for sustaining the compressive forces from the diseased blood vessels and ureters.

Considering these backgrounds, patterning of net-like patterns composed of many slit patterns alternately allocated in parallel to the pipe axis is investigated. To clarify the ultimate technological feasibility, stainless steel pipes with outer and inner diameters of 100 and 60  $\mu\text{m}$  were used as specimens. Although appropriate pipe diameters were 0.5-1 mm, such fine pipes were used instead depending on the limitations of exposure system.

## 2 LASER SCAN LITHOGRAPHY SYSTEM

Laser scan lithography system for delineating patterns on fine diameter pipes was developed in 2003 to fabricate various cylindrical micro-components with outer diameters of less than 500

μm. (Joshima et al., 2004) The technology was drastically improved by developing a new system in which a specimen pipe was held in the vertical direction. Specimen diameters were gradually reduced, and the minimum diameter size was reached to less than 50 μm. (Horiuchi and Sasaki, 2012) And, the system was used for fabricating micro-coil springs to give contact pressure forces to probe pins densely arrayed in circuit testers of semiconductor devices and bio-devices. (Horiuchi et al., 2012; Horiuchi et al., 2013)

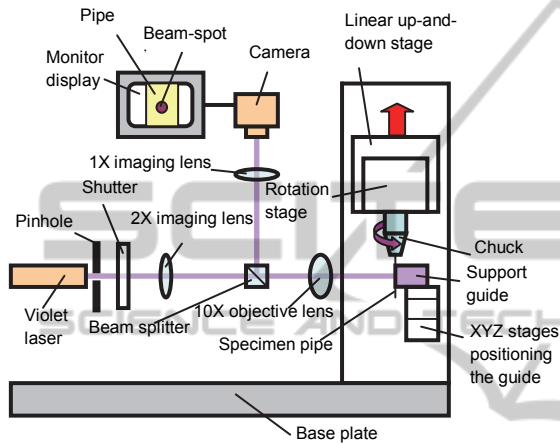


Figure 1: Fundamental structure of exposure system.

The fundamental structure of improved exposure system is shown in Fig. 1. In the system, laser beam is reshaped by a pinhole, and the light image of the pinhole exit is projected onto the surface of specimen pipe coated with a resist film. The projection ratio of the optics was calculated to be  $1/2 \times 1/10 = 1/20$  in total. The pipe specimen was supported by a mechanical chuck equipped to a rotation stage on an up-and-down stage, and scanned to the laser beam. By moving the specimen pipe, the resist film was scanned to the laser beam spot, and sensitized. The exposure beam spot on the specimen-pipe surface was monitored by projecting it on a monitor display.

Slit patterns were delineated by vertical linear scans of specimen pipes, and the specimen pipes were intermittently rotated for delineating parallel slit patterns one after another. As a resist, positive PMER P LA-900PM (Tokyo Ohka Kogyo) was used, and it was coated on the specimen pipes in approximately 3 μm thick using the dip method. (Joshima et al., 2004) This thickness was obtained by drawing specimens up at a speed of 0.8 mm/s.

### 3 CONTROL OF PATTERN-END PROFILES

#### 3.1 Swelling of Pattern Ends

Laser scans were controlled using a mechanical shutter, and open and shut operations were assigned by computer programs. At first, slit patterns were delineated according to the program that the specimen scan in the vertical direction was started just after the shutter was opened. Fig. 2 shows the patterns obtained by above mentioned method. The slit pattern length was 300 μm. It is known from the figures that the slit pattern ends swelled according to the increase of scan speed.

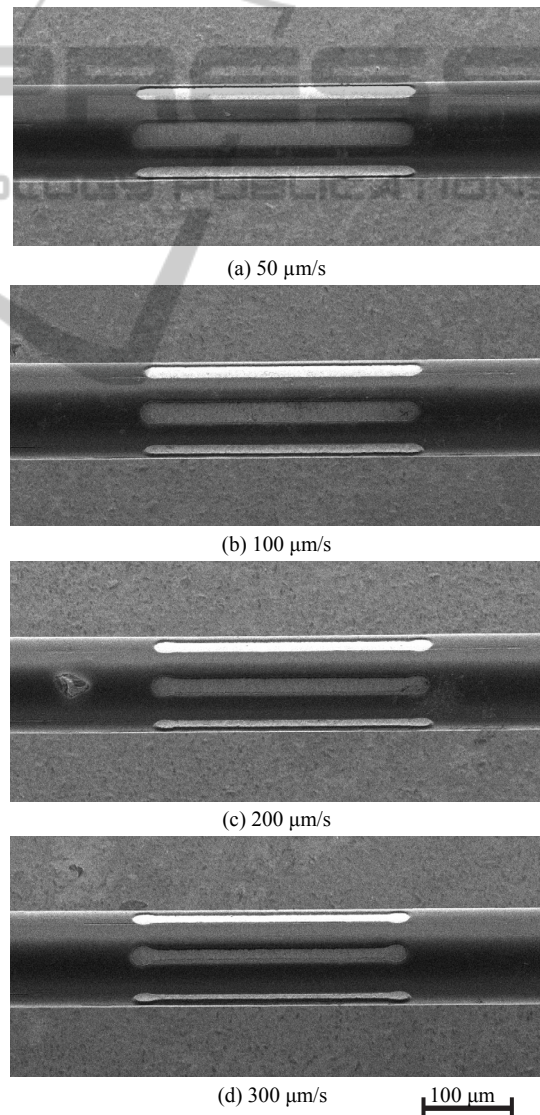


Figure 2: Slit patterns delineated by starting the scan of specimen pipe just after the shutter was opened.

Fig. 3 shows width changes along the patterns. It was clarified that the swells at the pattern ends became notable when the scan speed was more than 100  $\mu\text{m/s}$ .

It was considered that these swells of pattern ends were caused by the difference between the light beam intensity distributions of static spot exposure and dynamic scan exposure. Distribution of single-mode laser spot was roughly simulated by the Gaussian curve expressed by eq. 1.

$$I = I_0 e^{-2\left(\frac{r}{R}\right)^2} \quad (1)$$

Here,  $R$  is the beam radius and  $r$  is the radial distance from the beam centre. It is supposed that light intensity for the stopped spot exposures at the start and terminal points distributes according to this equation.

However, if the beam spot was scanned in  $x$  direction, exposure dose at the distance  $y$  from the centre line of the linear scan was decided by the area size  $S_y$  of the cross section of stereo beam intensity profile in the direction parallel to the scan direction  $x$ , as shown in Fig. 4.

The peak intensity  $I_y$  at the distance  $y$  is the same with that for the spot exposure, and estimated by eq. 1, if  $r$  is replaced by  $y$ . However, the cross section profiles are different depending on  $y$ , because the length  $L$  across the beam varies depending on  $y$ . That is, the length  $L_0$  at the centre is decreased to  $L_y$  at the distance  $y$ . When  $y$  becomes large,  $L_y$  steeply decreases. Accordingly,  $S_y$  steeply becomes small.

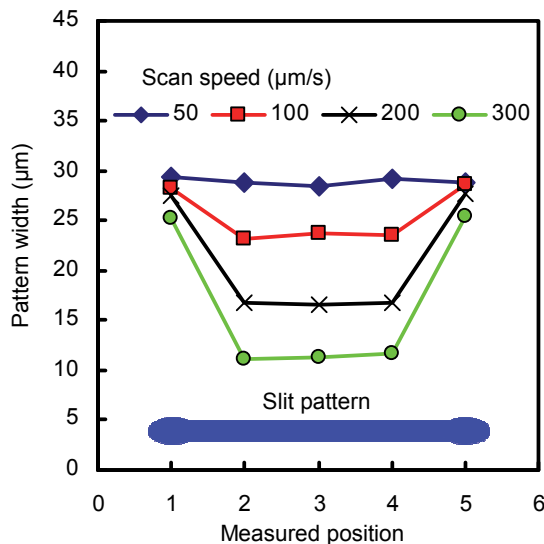


Figure 3: Width distribution of slit patterns delineated by starting to scan the specimen pipe just after the shutter was opened.

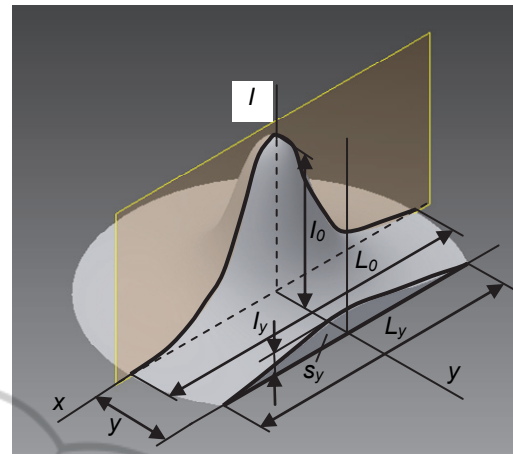


Figure 4: Figure for explaining parameters deciding the exposure dose of linear scan.

Because the exposure dose is proportional to  $S_y$ , the dose also steeply decreases at the side peripheries or at the places distant from the centre of scan lines. For this reason, the light intensity across the scan line distributes narrower than the static spot exposure. Accordingly, slit pattern widths become narrower than those at the pattern ends, and swells of pattern ends are generated.

### 3.2 Improvement of Pattern Profiles at Slit-pattern Ends

To improve swells at pattern ends, delineation method was improved, as shown in Fig. 5.

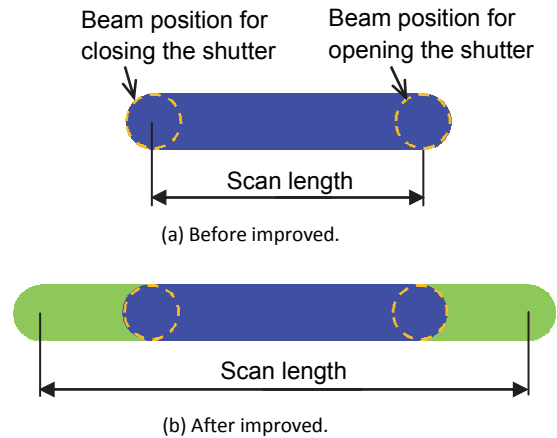


Figure 5: Improvement of timing for opening and closing the shutter.

In the conventional method shown in Fig. 5(a), the scan of specimen pipe was started just after the shutter was opened. On the other hand, in the improved method, patterns were delineated by

opening the shutter after the specimen pipes were scanned, as shown in Fig. 5(b). As a result, linear space patterns were delineated only by the genuine scan exposure. Results for the improved method are exhibited in Fig. 6.

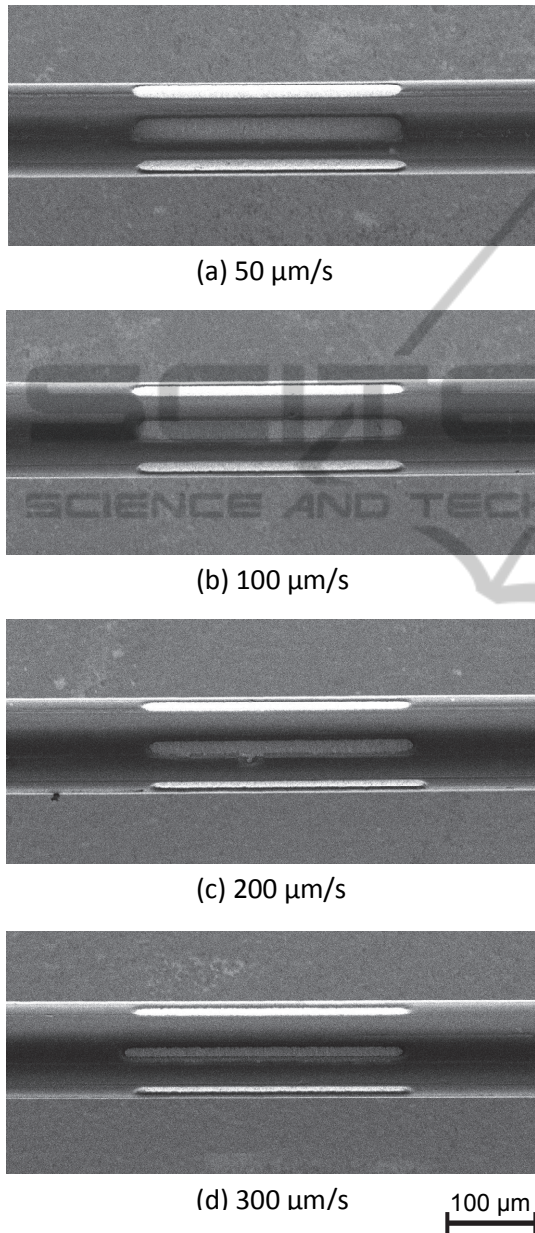


Figure 6: Slit patterns delineated by opening and closing the shutter during the scan of specimen pipes.

It was verified that swells at pattern ends were almost diminished by adding above mentioned approach and over scans. The width homogeneity is shown in Fig. 7. It was demonstrated that the straight space patterns with homogeneous widths were

obtained for various scan speeds. It was clarified that the mean space-pattern widths were intentionally changed by adjusting the scan speed in a wide range of 11-29  $\mu\text{m/s}$ , as shown in Fig. 8.

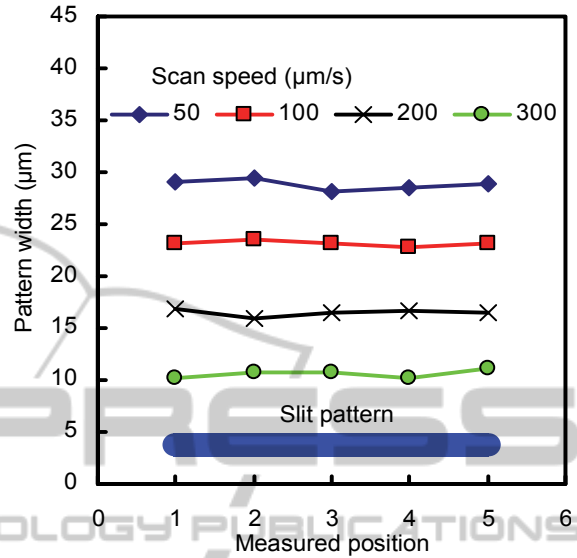


Figure 7: Width distribution of slit patterns delineated by opening and closing the shutter during the scan of specimen pipes.

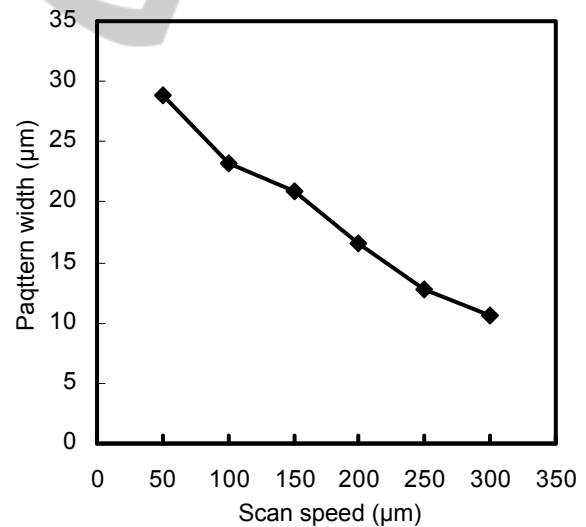


Figure 8: Space-pattern width dependence on scan speed.

#### 4 ALTERNATELY ALLOCATED SLIT PATTERNS

Next, alternately positioned slit patterns were delineated supposing the fabrication of net-like stents. Slit pattern positions were shifted by a half

pitch in the axial direction for every 90° rotation of the specimen axis. As a result, patterns shown in Fig. 9 were successfully delineated. Measured pattern widths were almost homogeneous, as shown in Fig. 10. If these patterns were delineated on a long pipe with appropriate diameters and the pipes were etched similarly to the patterns, aimed stents would be obtained.

It seems that the space-pattern widths are too narrow, and the resist-pattern widths are too wide. However, pipe walls are excessively etched according to the undercut phenomena. For this reason, space widths seem too narrow at a glance are probably appropriate for etching the pipes.

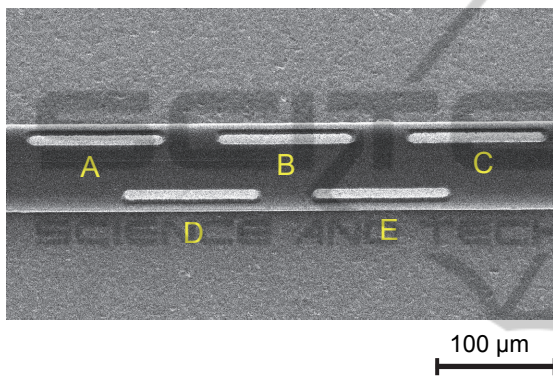


Figure 9: Alternately positioned slit patterns.

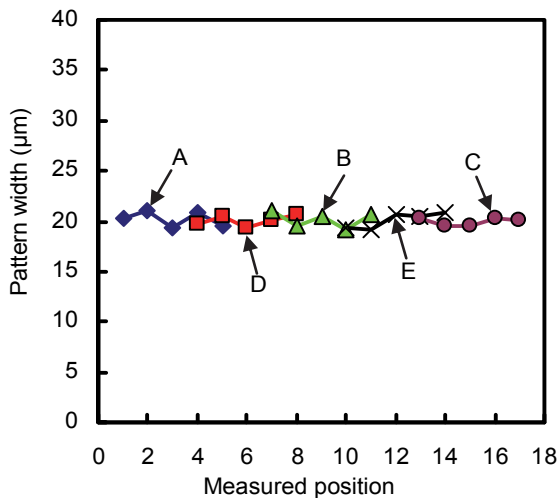


Figure 10: Width homogeneity of alternately positioned slit patterns.

### 5 IDEAS FOR IMPROVING PATTERNING SPEED

Slit patterning parallel to the specimen axis was

investigated. As a result, it was clarified that slit patterns with widths between 11 and 29 μm were successfully delineated, and pattern widths were sufficiently homogeneous. However, because the maximum delineation speed is 300 μm/s, it will take a long time to delineate practical stent patterns. The long patterning time is caused by the exposure principle of the system shown in Fig. 1. Because only one small laser spot is sequentially scanned on whole specimen surface, it takes a very long time.

This time, pipe specimens with an outer diameter of 100 μm were used, and by precisely delineating fine patterns even on such small diameter pipes, technical difficulty in patterning processes were almost cleared. The first reason why such fine pipes were used is the diameter limitation of specimen pipes attachable to the exposure system, and the second reason is the too long exposure times for delineating the slit patterns. Because the resist was coated in the parts of 20-mm near the specimen-pipe ends, it took approximately  $18 \text{ mm} / 300 \text{ μm/s} = 60 \text{ s} = 10 \text{ min}$  for delineating only one long slit pattern. Accordingly, it took  $10 \text{ min} \times 6 = 60 \text{ min} = 1 \text{ h}$  for delineating only 6 long slits on a 100-μm pipe. However, more complicated or larger volume patterning is required on specimen pipes with larger diameters of 0.5-1 mm. If such large diameter pipes were used, the total exposure time would become 5-10 h. Therefore, much faster exposure method is necessary.

As an exposure system for such use, scan projection exposure system shown in Fig. 11 will be effective. Original patterns on a reticle are projected onto a specimen pipe surface through a projection lens. By inserting an oblong slit aperture above the specimen, only patterns limited in a narrow region are printed on the almost flat top-surface of the specimen pipe. Therefore, the patterns are replicated clearly without being defocused. In addition, if the specimen pipe is rotated synchronously to linear scan movement of the reticle, all patterns on the flat reticle are printed on the whole cylindrical surface of specimen pipe.

Because patterns in the oblong exposure field are simultaneously printed on the specimen pipe, the total exposure time becomes far shorter than the laser scan lithography investigated here. Although the exposure time depends on the width of oblong slit, the light source power, and the optics for collecting the exposure light, it will be less than 1 min for a pipe with a diameter of 1 mm.

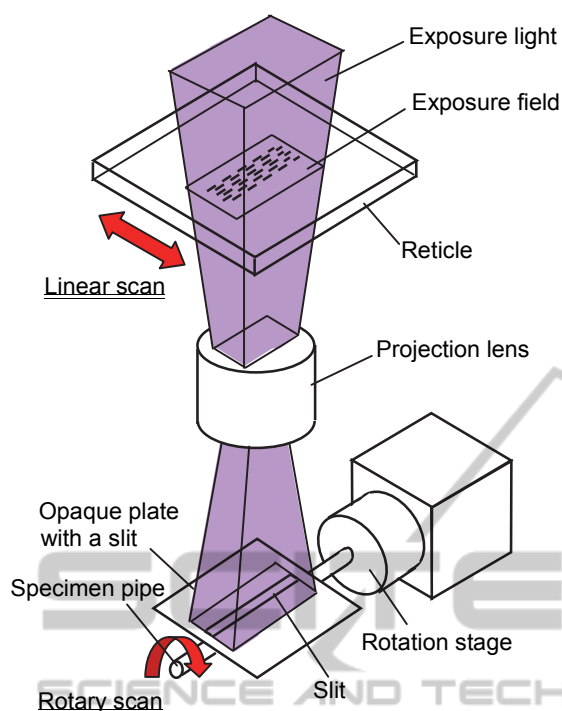


Figure 11: Scan exposure system with a high throughput using a lamp source and a reticle.

## 6 CONCLUSIONS

Slit pattern delineation on fine pipes were investigated for developing precise stents with diameters of less than 1 mm. As a result, fine slit patterns with widths of 11-29  $\mu\text{m}$  were delineated on fine stainless steel pipes with outer and inner diameters of 100 and 60  $\mu\text{m}$  using 3- $\mu\text{m}$  thick positive resist PMER LA-900PM.

By adding approach and over scans and controlling the exposure shutter appropriately, swells at pattern ends were almost diminished. As a result, slit patterns with homogeneous widths were obtained. In addition to simple parallel slit patterns, alternately allocated slit patterns were also homogeneously delineated.

Because a little long delineation time was anticipated, scan projection methods were also proposed as a counter measure. It is feasible to fabricate small diameter stents, if specimen pipes masked by the resist patterns are precisely etched.

## ACKNOWLEDGEMENTS

This work was partially supported by Grant-in-Aid

for Scientific Research (C) 26390040 from Japan Society for the Promotion of Science.

## REFERENCES

- Baichoo, E. and Wong Kee Song, L. M., 2014. Palliative enteroscopic stent placement for malignant mid-gut obstruction. *Gastrointestinal Intervention*, 3(1), pp. 30-34.
- Chandrasekhar, J., Allada, C., O'Connor, S., Rahman, M., Shadbolt, B., and Farshid, A., 2014. Efficacy of non-compliant balloon post-dilation in optimization of contemporary stents: A digital stent enhancement study. *IJC Heart & Vessels*, 3, pp. 43-48.
- Consentino, D., Zwierzak, I., Schievano, S., Diaz-Zuccarini, V., Fenner, J. W., and Narracott, A. J., 2014. Uncertainty assessment of imaging techniques for the 3D reconstruction of stent geometry. *Medical Engineering & Physics*, 36, pp. 1062-1068.
- Horiuchi, T., and Sasaki, R., 2012. New Laser-Scan Exposure Tool for Delineating Precise Helical Patterns onto Sub-50-Micron Wires, *Jpn. J. Appl. Phys.*, 51, 06FL01, pp. 1-5.
- Horiuchi, T., Ishii, H., Shinozaki, Y., Ogawa, T. and Kojima, K., 2012. Novel Fabrication Method of Microcoil Springs Using Laser-Scan Helical Patterning and Nickel Electroplating. *Jpn. J. Appl. Phys.*, 50, 06GM10, pp. 1-5.
- Horiuchi, T., Sakabe, H., Yuzawa, T. and Yamamoto, D., 2013. Fabrication of Straight Stainless-steel Microcoils for the Use of Biodevice Components. *Proc. 6<sup>th</sup> International Conference on Biomedical Electronics and Devices (BIODEVICES 2013)*, pp. 114-119.
- Hanada, K., Matsuzaki, K., Huang, X., and Chino, Y., 2013. Fabrication of Mg alloy tubes for biodegradable stent application. *Material Sci. and Eng. C* 33, pp. 4746-4750.
- Joshima, Y., Kokubo, T., and Horiuchi, T., 2004. Application of Laser Scan Lithography to Fabrication of Microcylindrical Parts. *Jpn. J. Appl. Phys.*, 43, pp. 4031-4035.
- Kumar, G. P., Cui, F., Danpinid, A., Su, B., Hon, J. K. F., and Leo, H. L., 2013. Design and finite element-based fatigue prediction of a new self-expandable percutaneous mitral valve stent. *Computer-Aided Design*, vol. 45, pp. 1153-1158.
- Wang, A., Eggermont, J., Dekker, N., Koning, P. J. H., Reiber, J. H. C., and Dijkstra, J., 2014. 3D assessment of stent cell size and side branch access in intravascular optical coherence tomographic pullback runs. *Computerized Medical Imaging and Graphics*, 38, pp. 113-122.
- Zhu, Y., Hu, C., Li, B., Yang, H., Cheng, Y., and Cui, W., 2013. A highly flexible paclitaxel-loaded poly ( $\epsilon$ -caprolactone) electrospun fibrous-membrane-covered stent for benign cardia stricture. *Acta Biomaterialia*, 9, pp. 8328-8336.